

THE BEAUTY OF LATTICE PERTURBATION THEORY: THE ROLE OF LATTICE PERTURBATION THEORY IN B PHYSICS

C.J. MONAHAN

*Department of Physics, College of William and Mary,
Williamsburg, VA 23187, USA
cjmonahan@wm.edu*

As new experimental data arrive from the LHC the prospect of indirectly detecting new physics through precision tests of the Standard Model grows more exciting. Precise experimental and theoretical inputs are required to test the unitarity of the CKM matrix and to search for new physics effects in rare decays. Lattice QCD calculations of nonperturbative inputs have reached a precision at the level of a few percent; in many cases aided by the use of lattice perturbation theory. This review examines the role of lattice perturbation theory in B physics calculations on the lattice in the context of two questions: how is lattice perturbation theory used in the different heavy quark formalisms implemented by the major lattice collaborations? And what role does lattice perturbation theory play in determinations of nonperturbative contributions to the physical processes at the heart of the search for new physics? Framing and addressing these questions reveals that lattice perturbation theory is a tool with a spectrum of applications in lattice B physics.

Keywords: Lattice QCD; lattice perturbation theory; automated perturbation theory; B physics; heavy quark physics.

PACS Nos.: 11.15.Ha, 12.38.Bx, 12.38.Gc

1. Introduction

Clarifying our understanding of B physics is an increasingly important undertaking in the hunt for Beyond the Standard Model (BSM) physics. The most recent round of experimental results from BaBar and the LHC have imposed strict bounds on possible BSM contributions to rare B decays ^{1,2,3,4,5,6,7,8}, whilst continued experimental and theoretical progress has lead to more exacting tests of Cabibbo-Kobayashi-Maskawa (CKM) matrix unitarity ^{9,10,11,12,13}.

Flavor-changing neutral current (FCNC) processes are forbidden at tree-level in the Standard Model of particle physics. Such processes can only proceed through loop contributions, which are sensitive to much higher energy scales than the b quark mass. FCNC decays therefore serve as a probe for BSM physics and can tightly constrain the nature and size of BSM interactions. In particular, precise measurements of the branching fractions of the rare $B_{(s)} \rightarrow \mu^+ \mu^-$ decays offer two of the most promising avenues for the detection of BSM effects. These decays are strongly sensitive to the existence of BSM particles in a variety of BSM scenarios (see, for example, the discussion and references in ¹). Semileptonic FCNC processes, such as $B \rightarrow K^{(*)} \mu^+ \mu^-$, may provide bounds on classes of BSM physics that are not ruled out by purely leptonic modes ^{6,14,15,16}.

Taking a different tack, the B sector also provides the opportunity for detecting BSM physics through precision tests of the unitarity of the CKM matrix. This matrix, which is unitary in

the Standard Model, relates the mass and weak-interaction eigenstates of down-type quarks and incorporates all the flavor-changing and CP-violating couplings in the Standard Model. A wide array of channels probe the CKM matrix, such as the semileptonic decays $B \rightarrow \pi \ell \nu$ and $B \rightarrow D^* \ell \nu$, and neutral B mixing. Combining independent determinations of each CKM parameter over-constrains the elements of the CKM matrix and discrepancies or deviations from unitarity may indicate the breakdown of the CKM framework. Currently a number of tensions at the $2 - 3\sigma$ level in unitarity fits hint at the exciting possibility of BSM physics^{9,10}.

Whether the hunt for BSM physics involves FCNC processes or CKM unitarity tests, one thing is clear: lattice quantum chromodynamics (QCD) is an indispensable tool in the search. Precision tests of the Standard Model require both precise experimental and theoretical inputs. Quarks are confined to color-singlet states and the physics of the weak interactions underlying FCNC decays and CKM-probing processes must be teased out from the dominant nonperturbative dynamics of the strong force. Lattice QCD is one of the most important tools presently available for precisely determining nonperturbative effects, but until recently has, in many cases, been playing catch-up with experimental precision. Over the last five years, however, the era of precision lattice QCD has dawned, with many results now at the few percent level^{17,18,19,20,21,22,23,24,25}. With the convergence of experimental and theoretical precision, and with growing experimental datasets and advancing lattice computations, tests of the Standard Model have become ever more exacting.

What is less clear, perhaps, is how lattice perturbation theory fits into the march toward high precision tests of the Standard Model. What is lattice perturbation theory? And what exactly is the role of lattice perturbation theory in the hunt for BSM physics? This review will answer these questions.

Viewed from the outside, Lattice QCD calculations are often seen as black boxes, simply non-perturbative number-crunchers that spit out *ab initio* predictions. Closer inspection reveals, not surprisingly, that this is not the whole story. I will attempt to lift the lid on heavy quark lattice QCD calculations — at least just a little — by examining the role of lattice perturbation theory in lattice B physics. I will frame this discussion in two ways: the first is the use of lattice perturbation theory in different formulations of heavy quarks on the lattice. Viewed through this lens, we see that lattice perturbation theory is a tool that is used, to varying degrees, by all the major lattice collaborations working on B physics. The second is the role of lattice perturbation theory in the calculation of specific physical processes, particularly key applications in the search for BSM physics. I focus on precision B physics; to this end I discuss not only processes currently in the headlights of BSM physics hunters, but also precision B spectroscopy, which has proved to be a trustworthy testing ground for lattice QCD and provides firm evidence that lattice QCD is indeed becoming more precise and reliable. For brevity I concentrate on the impact of lattice perturbation theory in lattice B physics, rather than discussing specific details of individual calculations.

I start by motivating lattice perturbation theory in Sec. 2 and then briefly review recent methods for automating lattice perturbation theory in Sec. 3. In Sec. 4 I examine the ways in which lattice perturbation theory is used in various heavy quark formulations on the lattice. I briefly discuss relativistic formulations for heavy quarks on the lattice, but focus on the historically more prevalent effective field theory approach and use this discussion to limn the limits of lattice perturbation theory. In the second half of the review I highlight some applications of lattice perturbation theory to specific physical processes at the forefront of BSM searches and conclude with a short summary

in Sec. 6.

2. Lattice perturbation theory

Lattice QCD is the preeminent approach for *ab initio* calculations of QCD processes and is conspicuously a tool for nonperturbative physics computations. In this view, the phrase “lattice perturbation theory” has the air of a contradiction — the perturbation theory of nonperturbative physics. But the phrase is slightly misleading: lattice perturbation theory is better viewed as “perturbation theory for lattice actions”. This move is not just cosmetic; the latter terminology is not only less outwardly troubling, but also generally more accurate and specific in scope. Unfortunately the new nomenclature is cumbersome; throughout this review I will continue to simply refer to lattice perturbation theory (henceforth “LPT”), with the understanding that what is really at the heart of the discussion is “perturbation theory for lattice actions”.

2.1. Motivating LPT

A glance at the LPT literature reveals a range of applications within lattice QCD: calculating the renormalization parameters of bare lattice actions; matching regularization schemes and extracting continuum results from lattice data; and improving lattice actions. These applications, however, are inter-related and can be broadly categorized as accounting for the physics of energy scales excluded by the lattice cutoff. In other words, each of these applications falls under the banner of renormalization.

Understanding these motivations for using LPT — that is, as a tool for renormalization — is also the key to understanding the justification for using lattice perturbation theory, laid out in ²⁶. The lattice serves as an ultraviolet regulator discretizing spacetime and excluding all momenta greater than π/a (where a is the lattice spacing). As we would in any other regularization scheme, we must calculate the renormalization parameters of the regularized theory to correctly account for high energy effects. In this case the excluded scales are those above the lattice cutoff, which corresponds to approximately 5 GeV for current lattice spacings. At these energy scales, the coupling constant is relatively small, $\alpha_s(\pi/a) \sim 0.2$, and perturbative approximations (and therefore LPT) are likely to be valid.

LPT thus provides the connection between the low and high energy regimes of QCD. Moreover, this connection has been tested and validated in a wide range of QCD processes by comparing higher order perturbative calculations with nonperturbative computations in the weak coupling regime ^{27,28,29,30,31,32,33}.

There is, however, some subtlety to this story: we must choose our coupling constant carefully to ensure the perturbative series is well-behaved. Early LPT calculations were plagued by slow convergence and inconsistent results ³⁴. These issues were the product of a poor choice of expansion parameter: the bare lattice coupling. We can greatly improve the convergence of our perturbative series by introducing an improved coupling constant, often defined in the “V-scheme” ³⁵, expressed at an appropriately chosen scale, the “BLM scale” ^{35,36}. In some cases, LPT is simply insufficient and nonperturbative renormalization is required (see Section 4.2 for an example).

Before turning to look at some of the uses of LPT in different lattice formulations, I will examine in a little more detail both renormalization and improvement in the context of LPT.

Renormalization and matching calculations In general one has two choices for calculating renormalization parameters, matching parameters or improvement coefficients for lattice actions: nonperturbative tuning or perturbative calculation. There are a variety of nonperturbative tuning methods. A full review is beyond the scope of this report, but a partial list includes step-scaling methods, which may be applied to the Schrödinger functional³⁷, off-shell Green functions (the “Rome-Southampton method”)³⁸ or physical quantities³⁹; imposing Ward identities or chiral symmetry relations⁴⁰; and fixing to physical quantities, such as meson masses, or relations, such as relativistic dispersion relations⁴¹.

Although these approaches differ considerably in practice, they share two particular advantages. All nonperturbative methods enable the replacement of perturbative truncation errors, which can be hard to quantify, with statistical and systematic errors, which can usually be determined reliably. In general, with intensified computational effort, these uncertainties can be systematically reduced. Secondly, a fully nonperturbative approach is the only truly *ab initio* method for QCD calculations.

Nonperturbative methods share a number of disadvantages as well: step-scaling and iterative methods incur a greatly increased computational expense, whilst matching to physical quantities results in a loss of predictive power.

LPT is an alternative to nonperturbative tuning. In this approach one calculates the renormalization constants or matching parameters perturbatively, carrying out the calculation in a spirit broadly similar to the standard perturbative calculations of continuum QCD. LPT is computationally much cheaper than nonperturbative tuning and there is no loss of predictive power. There are disadvantages, too, of course. Most notably LPT introduces perturbative truncation errors. As lattice calculations become more precise, the concomitant perturbative error often become the largest source of uncertainty in the result, which will ultimately necessitate multi-loop calculations will eventually be necessary. This is no mean feat: LPT is usually more involved than the corresponding calculations in continuum QCD. The relatively recent advent of sophisticated automated perturbation routines for lattice actions, however, means that multi-loop calculations for improved actions have been carried out^{42,43,44,45}. Despite the complications, the computational cost of such calculations is invariably lower than that for nonperturbative tuning, ensuring LPT is an attractive alternative to nonperturbative renormalization.

Improvement Precise lattice QCD computations generally require lattices with two properties: small lattice spacings to reduce discretization errors and large lattice volumes to remove finite size effects. Unfortunately lattice QCD calculations tend to be rather computationally expensive. And as the lattice spacing decreases and the lattice size increases, they grow ever more expensive.

Thankfully for precision B physics there is an alternative to simply using ever finer lattice spacings. Lattice actions can instead be “improved” to eliminate sources of error. The most common approach to improvement is the Symanzik improvement programme^{49,50}, in which scaling violations are systematically removed by adding irrelevant operators to the lattice action, organized by mass dimension. This approach is frequently significantly cheaper than simulating at smaller lattice spacings.

Determining the coefficients of the new terms in the improved action can usually be carried out quite simply at tree-level, but for precision studies, this is insufficient. By construction lattice actions exhibit the same long-range physics as continuum QCD, but their short-range behaviour is

distorted by the lattice cutoff. Radiative corrections to the new operators in the action renormalize the coefficients away from their tree-level values and this can lead to new sources of uncertainty in lattice predictions. By matching onshell quantities on the lattice and in the continuum, the resultant discrepancies can be removed order-by-order in perturbation theory.

There is naturally a price to be paid for adding extra terms to the action (radiatively improved or otherwise). The extra operators considerably complicate the Feynman rules for the improved actions. Highly improved actions, such as the HISQ and NRQCD actions that I discuss in Sec. 4, generate Feynman rules that cannot feasibly be manipulated by hand. Furthermore, the lack of Lorentz symmetry complicates the evaluation of Feynman integrals, which are no longer amenable to Feynman parameter transformations or the other tricks of the continuum trade and must be handled numerically. To cope with these complications LPT has been automated.

3. LPT today: Automation

In recent years a number of automated lattice perturbation theory algorithms have been developed, many following the pioneering work of Lüscher and Weisz⁵¹. An early variant of the Lüscher-Weisz (LW) algorithm was deployed in^{42,52,53}, but currently the most widely used descendant of the LW algorithm is implemented in the HIPPY/HPSRC software packages^{54,55}. More recently, the LW algorithm was adapted for gauge actions in the Schrödinger functional scheme⁵⁶. A new software package, called `pastor`, has extended this work to include Wilson-type relativistic quarks and HQET heavy quarks⁵⁷. Initial calculations with `pastor` are underway^{58,59}. Finally, following an altogether different approach, a computer algebra system has been constructed and optimized for LPT⁶⁰. Although the use of this software has so far been restricted to a calculation using the relativistic heavy quark action in the Columbia formulation⁴¹, in principle the algorithm can be extended to any lattice quark action.

The HIPPY/HPSRC software packages have now been used in a variety of perturbative calculations, for example in^{18,31,61,62,63,64,65}, and extensively tested against previous results. Evaluating Feynman integrals is a two stage process with the HIPPY/HPSRC routines: one first generates the Feynman rules with HIPPY, a set of PYTHON routines that encode the Feynman rules in “vertex files”. These vertex files are then read by the HPSRC FORTRAN modules, which evaluate the corresponding integrals numerically via the VEGAS algorithm⁶⁶ or exact mode summation over a finite lattice. Any derivatives required in the calculation are implemented analytically using the derived `taylor` type, defined as part of the FORTRAN `Taylor` package⁶⁷. Both HIPPY and HPSRC implement parallel processing using MPI (Message Passing Interface).

The Schrödinger functional scheme has been widely used over the last thirty years (see the Sec. 4.2 for references). The advent of LPT for the Schrödinger functional scheme is, however, much more recent. There are two reasons for this: the first is the additional complexity introduced by the Schrödinger functional formalism and the second is that LPT has very limited application to HQET computations, as I discuss in more detail in the next section. LPT is nevertheless useful, because perturbative calculations can serve as a starting point for more precise nonperturbative methods. These nonperturbative methods are computationally expensive and there are a large number of renormalization parameters in the Schrödinger functional scheme, many of which have only a small relative effect on the final result. Perturbative investigations can guide where computational

resources should be focussed to most improve the precision of lattice calculations.

There are three complications that must be handled by automated routines for the Schrödinger functional scheme. Firstly, translational invariance, which is assumed in the `HiPPY/HPsrc` algorithm, is broken in the time direction. Secondly, we must account for an induced abelian color background gauge field^a. Thirdly, at a given order in the coupling constant, there are extra diagrams generated by the boundary conditions of the Schrödinger functional scheme that are not present in other lattice formulations. The `pastor` software package, written specifically to deal with these difficulties, is based on `C++` routines that generate vertices and a `PYTHON` frontend wrapper that allows the user to specify the lattice actions in symbolic form in `C++`. An `xml` input file specifies the desired observable in the Schrödinger functional scheme, which the `PYTHON` frontend routine parses to generate all the relevant diagrams of order g_0^2 . These diagrams are then evaluated with a `C++` program generated by the `PYTHON` wrapper^{57,58}.

The most recent automated LPT framework, presented in⁶⁰, is based on a new `C++` computer algebra library optimized for lattice perturbation theory. Lattice actions are defined by `C++` classes that allow the user to specify the action in text form. These classes extract the vertices, then further `C++` classes perform Wick contractions and convert the algebraic representation of the integrand into efficient `C++` code that can be evaluated numerically. This framework also contains routines that can perform analytic differentiation with respect to the external momenta and undertake continuum calculations in dimensional regularization using the Passarino-Veltman reduction⁶⁸.

4. LPT today: Applications in heavy quark lattice formulations

The computational expense of lattice QCD has been a distinct problem for b quarks, which are heavy and therefore “fall through” lattices that are too coarse to accurately resolve the Compton wavelength of the b quark. Putting this more precisely: it is not currently computationally feasible to use lattices large enough and fine enough to simultaneously satisfy $m_\pi L \gg 1$ and $m_b a \ll 1$. Here m_π is the mass of the lightest propagating particle in the theory; L is the side length of the lattice; and m_b is the mass of the b quark. Heavy-light systems, which feature heavily in BSM searches in the B sector, represent the worst of all computational worlds; they are characterized by both the mass of the light quark and the b quark — scales separated by several orders of magnitude.

Lattice QCD has traditionally dealt with this problem using the technology of effective field theories. Despite the considerable advances in computing infrastructure and simulation algorithms over the last thirty years, even state-of-the-art lattice computations require extrapolations up to the b quark mass^{23,46,47,48} and effective field theories continue to play an important part in lattice simulations.

Historically, the application of effective field theoretic techniques to lattice QCD has elucidated the interplay of perturbative and nonperturbative physics and has consequently helped advance the understanding of conceptual issues such as the operator product expansion and the role of renormalons. I will examine effective theories for heavy quarks more closely to highlight some of the limitations of LPT,

^aIn fact, the `HiPPY/HPsrc` packages have been extended to use background field gauge⁶⁵, but this implementation is not sufficient for the Schrödinger functional scheme.

There are two widely used approaches to heavy quarks on the lattice: nonrelativistic QCD (NRQCD) and heavy quark effective theory (HQET). Both take advantage of the large mass of the b quark relative to other scales in QCD physics and both have the same infinite mass, or stationary quark, limit. There are, however, important differences. Here I only briefly outline some of the important considerations for LPT for both lattice NRQCD and HQET. For a more complete pedagogical introduction to continuum NRQCD, see, for example, ⁶⁹. Reviews of HQET in the continuum appear in ⁷⁰ and in the textbooks ^{71,72}, whilst lattice HQET is reviewed in ⁷³.

4.1. NRQCD

Heavy quark bound states are typified by the small relative velocity of their constituent quarks. In heavy $b\bar{b}$ states, such as the η_b and Υ mesons, this relative velocity is approximately $v^2 \simeq 0.1$. Consequently, v induces three well-separated energy scales: the mass, $\mathcal{O}(m_b)$; the momentum, $\mathcal{O}(m_b v)$; and the kinetic energy $\mathcal{O}(m_b v^2)$. NRQCD is also suitable for heavy-light systems, such as the B and B_s mesons, in which case the expansion parameter is Λ_{QCD}/m_b and the power counting is that of HQET, but for simplicity I restrict my discussion to heavy-heavy systems.

To construct the NRQCD action we use the Foldy-Wouthuysen-Tani transformation ⁷⁴ to decouple the quark and antiquark fields and undertake a nonrelativistic expansion. The result is an effective theory with nonrelativistic, low-energy degrees of freedom. At lowest order, the continuum NRQCD action is just the nonrelativistic Schrödinger action.

Following the Symanzik improvement scheme, we can then systematically include interactions and improve the NRQCD action to a given order in v and Λ_{QCD}/m_b by adding irrelevant higher order operators. Finally, armed with an appropriately improved continuum NRQCD action, we then discretize it for lattice computations. We must choose the coefficients of the higher order operators to ensure the effective lattice theory replicates the correct behaviour for physical observables. As I discussed in the previous section, calculating the radiative corrections to the improvement coefficients is the role of LPT.

One property of lattice NRQCD is a particular challenge: lattice NRQCD is a nonrenormalizable effective theory with no continuum limit. We cannot take the limit of vanishing bare lattice mass, $am_b \rightarrow 0$. Even at leading order in the Foldy-Wouthuysen-Tani transformation, the $1/(am_b)$ corrections are present in the heavy quark propagator. Interaction and improvement terms in the NRQCD action are higher order in $1/(am_b)$ and consequently there are an infinite number of divergences that cannot be absorbed into the renormalization parameters.

From a perturbative standpoint, this means the series that define the radiative corrections to the higher order operators in the action become ill-defined at small masses. LPT — and indeed NRQCD — fails in the region $am_b \leq 1$. This has been explicitly demonstrated for the case of the chromomagnetic correction to NRQCD by studying the mass dependence for a range of masses around $am_b = 1$ ⁷⁶. We can safely use LPT to improve lattice NRQCD, provided we remain in the region for which $am_b > 1$. This ensures that nonperturbative computations using lattice NRQCD converge with those obtained from continuum QCD.

Although we can not take the continuum limit of lattice NRQCD — it does not exist — we can nevertheless extract continuum results from lattice NRQCD calculations. By carrying out computations at different values of the lattice spacing within the region of validity of NRQCD, *i.e.* at different

values of am_b for $1/m_b < a < 1/\Lambda_{\text{QCD}}$, we may parameterize the lattice spacing dependence of our results and quote uncertainties appropriately. With sufficient improvement, we can reduce the lattice spacing dependence to, for example $\mathcal{O}(1/(am_b)^2)$ or higher, and obtain correspondingly precise results, often at the few percent level. Without LPT, such precise nonperturbative results for many B physics parameters would be a distant hope for the future.

4.2. HQET

Although HQET bears many similarities to NRQCD, the approach is both conceptually and practically distinct. The first conceptual difference is that, unlike NRQCD, HQET is an effective theory for singularly heavy hadrons; mesons such as the Υ or η_b are off limits. The second crucial distinction is that HQET is believed to be renormalizable at leading order, *i.e.* in the infinite heavy quark mass, or “static”, limit. The third contrast is that, even in the static limit, the renormalization and matching parameters of lattice HQET must be calculated nonperturbatively for precise B physics results⁷⁷. LPT will not do.

HQET is motivated by the intuition that singularly heavy hadrons are analogous to a hydrogen atom, with the b quark playing the part of the proton and the light quark the electron. Constructing HQET follows the same effective field theory approach to building NRQCD: we identify the relevant degrees of freedom, decouple the high and low energy modes via the Fold-Wouthuysen-Tani transformation and include all terms consistent with the desired symmetries at a given order in the expansion. We start by building an effective field theory that describes the light degrees of freedom interacting with a static color source, the heavy quark. Then, rather than including higher order operators directly in the HQET Lagrangian, we expand the non-leading terms in the path integral weight factor, $\exp(-S_{\text{HQET}})$, so that the non-leading contributions appear as insertions in correlation functions. More explicitly, we write

$$\begin{aligned} \exp(-S_{\text{HQET}}) &= \exp \left[-a^4 \sum_x \left(\mathcal{L}_{\text{HQET}}^{\text{static}}(x) + \mathcal{L}_{\text{HQET}}^{(1)}(x) \right) \right] \\ &= \exp \left[-a^4 \sum_x \mathcal{L}_{\text{HQET}}^{\text{static}}(x) \right] \left(1 - a^4 \sum_x \mathcal{L}_{\text{HQET}}^{(1)}(x) \right), \end{aligned} \quad (1)$$

where $\mathcal{L}_{\text{HQET}}^{\text{static}}$ is the leading order HQET Lagrangian and $\mathcal{L}_{\text{HQET}}^{(1)}$ contains higher order terms. This approach ensures that HQET remains renormalizable and the continuum limit of HQET correlation functions exists, provided all local operators at a given order in $1/(am_b)$ are included.

The parameters of the effective theory are fixed at tree-level by the FWT transformation, but beyond tree-level these must be found by matching to a $1/m_b$ expansion of continuum QCD. Perturbative matching is insufficient for precision B physics. Continuum HQET matching factors have been perturbatively studied in, for example,⁷⁸ where it was demonstrated that even at three-loops the convergence of the perturbative series is very slow. The matching coefficients are scale dependent, and their magnitude can be reduced by lowering the scale, but this does not help: at the scale at which the perturbative series converges quickly the coupling constant itself is rather large. There seems to be no escaping the conclusion that for reliable results at the precision of a few percent, nonperturbative matching is necessary⁷³.

Beyond leading order, matrix elements of higher dimensional operators mix and their coefficients must be fine tuned. These operators diverge with inverse powers of the lattice spacing and attempting to remove these power divergences via perturbative matching introduces ambiguities associated with so-called “renormalons”. A full study of renormalons and their role in HQET would take us too far from our central topic; for in-depth reviews with applications to B physics and HQET, see for example, ^{79,80,81}. In essence renormalons arise because perturbative QCD is an asymptotic approximation to QCD that fails to capture nonperturbative behavior. A common example is the pole mass, which is a long distance quantity that can be rigorously defined order-by-order in perturbation theory as the pole of the renormalized quark propagator, but is subject to inescapable renormalon ambiguities of $\mathcal{O}(\Lambda_{\text{QCD}}/m_b)$ when nonperturbative effects are included ^{82,83}.

For our purposes, though, the central point is that renormalization parameters of HQET must be calculated nonperturbatively. This is a non-trivial task to implement for precision B physics, because one must ensure firstly that the HQET expansion is sufficiently accurate and secondly that the numerical precision is adequate. On top of this, the lattice simulations must be undertaken with physical volumes large enough to avoid significant finite volume corrections. Currently the ALPHA collaboration is carrying out a programme of precision B physics using HQET for the b quark ^{24,25,84,85,86} and implementing nonperturbative renormalization using the Schrödinger functional scheme and a step-scaling method ^{87,88}.

All this does not mean, however, that LPT has no role to play in HQET computations. In fact, the ALPHA collaboration has recently developed automated LPT routines for the Schrödinger functional scheme ^{57,58} to serve as an exploratory guide to focus computational effort most efficiently in nonperturbative determinations.

4.3. Relativistic heavy quark actions

Relativistic heavy quark actions combine aspects of effective theories and fully relativistic treatments and hence serve as a suitable framework for both light and heavy quarks ^{89,90,91}. The basic idea of the relativistic heavy quark formalism is to extend the Symanzik effective theory approach, on which NRQCD and HQET are based, to include interactions from both the small $m_q a$ and large m_q/Λ_{QCD} limits. As we take the limit of vanishing bare mass, $m_q a \rightarrow 0$, the relativistic heavy quark action reduces to the $\mathcal{O}(a)$ -improved clover action ⁹². Conversely, in the large bare mass limit, when $m_q \gg \Lambda_{\text{QCD}}$, the action breaks the time-space axis interchange symmetry and can be interpreted nonrelativistically, with a universal static limit.

Both the Fermilab Lattice/MILC collaboration and the RBC/UKQCD collaboration, currently employ relativistic heavy quarks for precision B physics ^{22,41}. These collaborations’ approaches to the relativistic heavy quark formalism differ primarily in the methods they use to tune their actions.

The RBC/UKQCD method uses three physical conditions to tune their parameters, matching to the spin-averaged B_s mass and hyperfine splitting and ensuring the continuum dispersion relation holds for the B_s meson. This tuning process is nonperturbative, but there is nonetheless a role for LPT. Perturbative calculations of the three tuning parameters at one-loop have been carried out to provide a consistency check for the nonperturbative tuning process ^{41,60}. Ultimately LPT will be used for parameters for which nonperturbative tuning is not available.

In the Fermilab approach, two of the parameters are fixed and the third tuned nonperturbatively, using the spin-averaged B_s mass⁹³. LPT played its part in the original construction of the Fermilab action⁸⁹, and remains an important component for matching lattice matrix elements to their continuum counterparts. For decays such as the semileptonic $B \rightarrow \pi \ell \nu$ and $B \rightarrow D \ell \nu$ decays, the Fermilab Lattice/MILC collaboration use a mixed approach to matching. The bulk of the matching is carried out nonperturbatively, leaving a factor close to unity that can be calculated perturbatively^{94,95,96,97}. For other processes, such as neutral B mixing, however, the Fermilab Lattice/MILC collaboration uses a purely perturbative matching procedure²².

Finally, it is worth noting that LPT played a critical role in the formulation of the relativistic heavy quark action used by the Tsukuba group⁹⁰. In this formulation, there is an extra parameter in the action that cannot be nonperturbatively determined⁹⁸.

4.4. Fully relativistic b quarks: HISQ and twisted mass fermions

Two lattice collaborations have recently begun to implement a programme of precision B physics using purely relativistic actions: the HPQCD collaboration^{46,47,48} and the ETM collaboration^{23,99,100}.

These collaborations use different relativistic actions in their computations, but both presently require extrapolations up to the physical b quark mass. The HPQCD collaboration uses the highly improved staggered quark (HISQ) action¹⁰¹, whilst the ETM collaboration employs a twisted mass variant of the Wilson action. The HISQ action exhibits exact chiral symmetry in the massless limit and therefore the heavy-light axial-vector and vector currents are absolutely normalized and do not require operator matching. The role of LPT in HISQ calculations is consequently somewhat reduced, but not completely absent. One loop calculations were required in the construction of the HISQ action. Furthermore, renormalization parameters for the tensor current and four quark operators are not absolutely normalized and therefore require matching to their continuum counterparts.

The ETM collaboration uses nonperturbative renormalization for the quark bilinear operators used in B physics applications¹⁰². Nevertheless, LPT is used to parameterize the discretization errors associated in the scale dependence of the nonperturbative renormalization factors in the RI-MOM scheme¹⁰³. Subtracting the one-loop perturbative behaviour significantly improves the size of discretization errors in the renormalization constants¹⁰⁴. The part that LPT plays here may be restricted, but it has still been important in improving the precision of twisted mass computations.

As above discussion makes clear, even as nonperturbative simulations move closer to the ideal of true *ab initio* calculations of QCD processes, LPT retains a vital role in extracting precise results. To clarify this role further, I now turn to the application of LPT in specific B physics processes.

5. LPT today: Applications in B physics

A handful of key B processes have become the loci of considerable experimental and theoretical attention. Effort has naturally focused on those processes that have, or are likely to soon have, small experimental and theoretical uncertainties. I will concentrate on only those channels that lie at the heart of the searches for BSM physics and CKM matrix unitarity violation and restrict my discussion to exclusive channels. Inclusive processes, whilst playing a vital role in BSM searches and constraining CKM matrix unitarity, fall outside the scope of this short review.

I summarize the processes in which LPT has been an important ingredient in Table 1. I break the table into three sections: in the top third I tabulate the key processes currently in the headlights of the flavor physics community. In the second third I present other processes for which LPT has been necessary for precise nonperturbative results. These processes have yet to achieve the experimental or theoretical importance of the processes listed in the first third of the table (usually because of larger experimental or theoretical uncertainties), but are nevertheless playing an increasingly important role in flavor physics in the heavy quark sector. In the final third, I present some more speculative approaches to uncovering new physics. Such processes are either poorly understood theoretically or are yet to be observed experimentally.

Naturally this hierarchy is largely a difference of degree rather than difference in kind, but highlights the crucial processes at the center of current BSM searches. Within Table 1 I distinguish between processes that determine CKM matrix elements, and thereby constrain CKM matrix unitarity, and rare decays that offer hope for detection of BSM loop effects. I represent this distinction in the second column. In the third column I give the quantity determined by lattice QCD that characterizes the nonperturbative physics of the process. In column four I list the relevant renormalization parameters calculated using LPT. I use the shorthand Qq to represent heavy-light currents, QQ for heavy-heavy currents and $QQqq$ to indicate four-fermion interactions.

Table 1. Summary of B physics processes discussed in this article. For a full description of the table, see the accompanying text.

Process	B physics	Lattice parameter	Renormalization (LPT)	Refs.
$B \rightarrow \pi \ell \nu$	V_{ub}	form factors	Qq vector current	62,97,115,123
$B \rightarrow D^* \ell \nu$	V_{cb}	form factors	QQ vector current	97,115,118,120
$B_s \rightarrow \mu^+ \mu^-$	rare decay	decay constant	Qq axial-vector current	97,115,123
$B_q^0 - \bar{B}_q^0$ mixing	V_{td}/V_{ts}	$SU(3)$ breaking ratio	$QQqq$ operator	131,134,135
$B \rightarrow \tau \nu$	V_{ub}	decay constant	Qq axial-vector current	97,115,123
$B \rightarrow D \ell \nu$	V_{cb}	form factors	QQ vector current	97,115,118,120
$B \rightarrow K \ell^+ \ell^-$	rare decay	form factors	Qq vector current	62,115,123
$B \rightarrow K^* \gamma$	rare decay	form factors	Qq tensor current	62
$B \rightarrow X_u \ell \nu$	V_{ub}	form factors	Qq vector current	62,97,115,123
$B_s \rightarrow K \ell \nu$	V_{ub}	form factors	Qq vector current	62,115,123
$B_c \rightarrow \tau \nu$	V_{cb}	decay constant	QQ axial-vector current	97,115,118

5.1. Heavy-light current renormalization

Matrix elements of quark currents are the starting point for any lattice computation of nonperturbative QCD contributions to weak interaction processes. Understanding quark current renormalization is consequently a critical component of precise lattice QCD predictions.

The vector current mediates weak interactions between states of the same parity, such as the semileptonic decay $B \rightarrow \pi \ell \nu$, which is parameterized by

$$\langle \pi | V^\mu | B \rangle = f_+(q^2) \left[p_B^\mu + p_\pi^\mu - \frac{m_B^2 - m_\pi^2}{q^2} q^\mu \right] + f_0(q^2) \frac{m_B^2 - m_\pi^2}{q^2} q^\mu, \quad (2)$$

where f_+ and f_0 are the “form factors”. In the limit $m_\ell \rightarrow 0$, a good approximation for electron and muon neutrinos, the decay rate reduces to

$$\frac{d\Gamma}{dq^2} \propto |V_{ub}|^2 |f_+(q^2)|^2. \quad (3)$$

This channel lies at the center of one of the main tensions in analyses of CKM matrix unitarity: currently, the values of V_{ub} from inclusive and exclusive semileptonic decays exhibit a 3.3σ disagreement¹⁰.

Other semileptonic B modes, such as $B \rightarrow \rho\ell\nu$, $B \rightarrow \eta\ell\nu$ and $B \rightarrow \omega\ell\nu$, represent rather more speculative possibilities for the extraction of V_{ub} . The study of such decays is currently in its infancy for lattice QCD (see, for example,¹⁰⁵ for a discussion of some of the challenges), but in principle any independent measurement offers the opportunity for greater understanding of the CKM mechanism. Similarly, the $B_s \rightarrow K\ell\nu$ provides another exclusive determination of V_{ub} and is currently being explored on the lattice¹⁰⁶, in advance of experiments proposed at LHCb¹⁰⁷ and Belle¹⁰⁸.

Purely leptonic decays of pseudoscalars, such as $B \rightarrow \ell\nu$, are directly sensitive to V_{ub} and therefore offer further insight into this tension. Such decays require a spin-flip, however, and the decay rate is helicity-suppressed by m_ℓ^2/m_B^2 . Only the $B \rightarrow \tau\nu$ mode has been observed¹⁰⁹. Consequently the experimental uncertainty of the branching ratio prevents determinations of V_{ub} from reaching the precision achieved with the semileptonic modes. In addition, the leptonic decay $B \rightarrow \tau\nu$ is expected to be sensitive to the presence of a charged Higgs boson, which is an exciting opportunity for experimentalists, but means that determinations of V_{ub} from this process may be difficult to interpret in terms of explicit unitarity violation. Nevertheless, experimental uncertainties will decrease and precise lattice computations will ensure that leptonic decays can ultimately deepen our understanding of the V_{ub} discrepancy.

Furthermore, the decay constants that parameterize leptonic decays are crucial ingredients in indirect searches for BSM physics. Observation of the rare $B_{(s)} \rightarrow \mu^+\mu^-$ decays is one of the key aims of the LHC. The high sensitivity of these processes to BSM physics ensures that they are amongst the star contenders for “likeliest channel for new physics results”. The branching fractions of these rare decays are proportional to the square of the decay constants, $f_{B_{(s)}}$, defined via the matrix elements of the leptonic decays $B_{(s)} \rightarrow \ell\nu$ as

$$\langle 0|A_0|B_{(s)}\rangle = f_{B_{(s)}} M_{B_{(s)}}, \quad (4)$$

where A_0 is the temporal component of the axial-vector current and $M_{B_{(s)}}$ the mass of the $B_{(s)}$ meson. Although the decay channel $B_s \rightarrow \ell\nu$ is not a physical process, it is nonetheless a process that can be computed within lattice QCD. In fact, the most precise values for the branching fraction of $B_{(s)} \rightarrow \mu^+\mu^-$ are obtained by taking a ratio with the $B_s^0 - \overline{B}_s^0$ mixing mass difference, ΔM_s ¹¹⁰. In this case, the dependence on f_{B_s} drops out. Determinations using both methods have been remarkably consistent, providing a strong check of the reliability of lattice computations, because the lattice calculations for B_s decays and $B_s - \overline{B}_s$ mixing are rather different.

Precise determinations of form factors and decay constants from lattice QCD are therefore of paramount importance in the hunt for BSM physics. And this is where LPT steps into the fray. The most up-to-date determinations of form factors and decay constants come from four lattice collaborations using four different formalisms. The ETM collaboration employ twisted mass

fermions with $n_f = 2$ species of sea quarks (with $n_f = 2 + 1 + 1$ calculations underway)²³, whilst early results from the ALPHA collaboration on $n_f = 2$ ensembles with $\mathcal{O}(a)$ -improved Wilson fermions are now available^{111,112}. The Fermilab Lattice/MILC group^{113,114} and the HPQCD collaboration both use staggered fermion ensembles generated by the MILC collaboration, with different valence quark actions. The HPQCD collaboration has examined a wide range of flavored and unflavored meson decay constants. The current status of the decay constant “spectrum” from the HPQCD collaboration is illustrated in Fig. 5.1 and demonstrates the excellent agreement with experimental data.

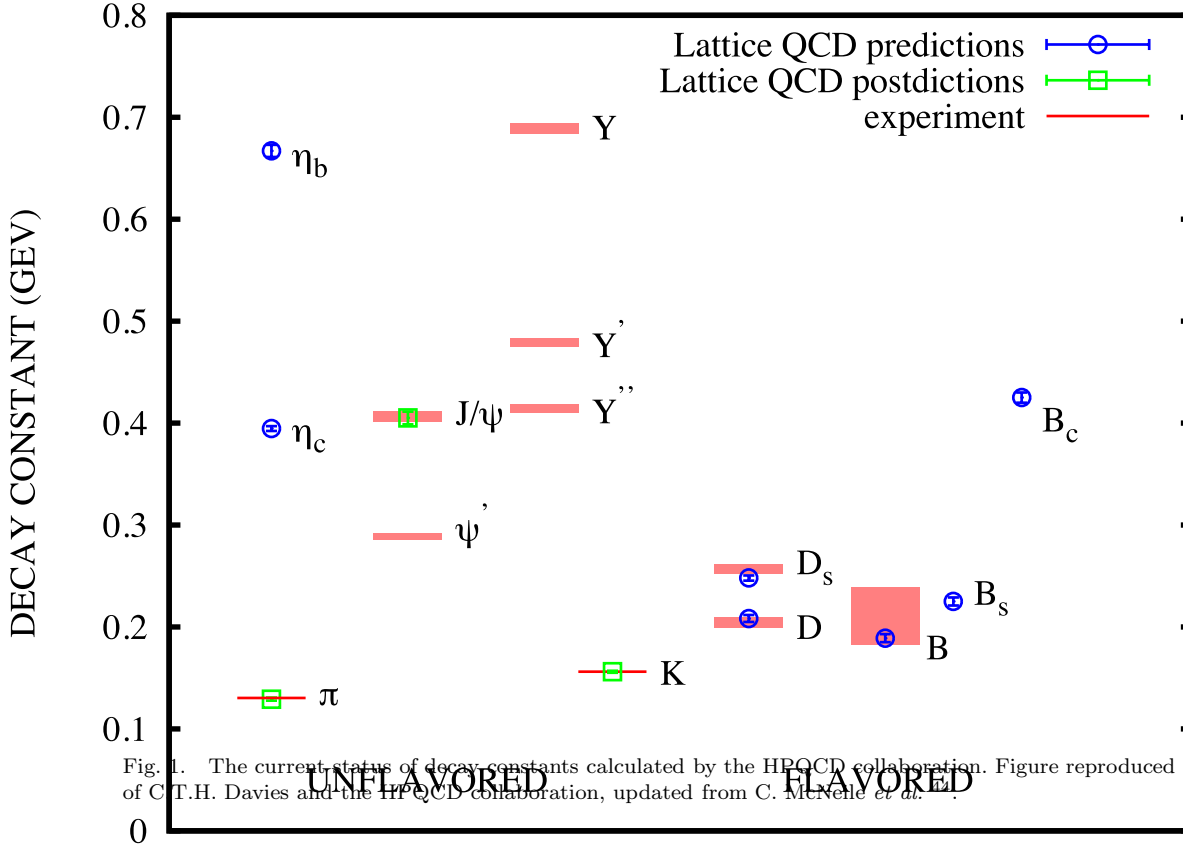


Fig. 1. The current status of decay constants calculated by the HPQCD collaboration. Figure reproduced courtesy of C.T.H. Davies and the HPQCD collaboration, updated from C. McNeile *et al.*

All four collaborations use LPT, albeit to varying degrees. The HPQCD collaboration has made heavy use of LPT in recent computations, so I turn now to an example for the quark currents used by the HPQCD collaboration.

5.1.1. A physics example: LPT in the HPQCD approach

The HPQCD collaboration has determined both the decay constants f_B and f_{B_s} ^{47,19,115} and the form factors f_+ and f_0 ^{116,117}. These determinations fall into two classes: the more traditional calculations use nonrelativistic b quarks paired with relativistic staggered light quarks whilst recent computations have pioneered a completely relativistic treatment of the b quarks using the

HISQ action. This entirely relativistic approach has several advantages that significantly improve the precision of the computation; the resulting value, $f_{B_s}^{\text{HISQ}} = 0.225(4)$ GeV⁴⁷, is the most precise currently available. Using relativistic b quarks avoids any need for effective actions and their associated systematic uncertainties, and the HISQ action has an absolutely normalized axial-vector current, removing the requirement for renormalization parameter calculations.

This approach does not make LPT redundant, however. Simulations with relativistic b quarks are yet to reach the physical point and a determination of f_B is even more computationally demanding. Lattice calculations with NRQCD remain the most competitive method for determining the ratio f_B/f_{B_s} . Systematic uncertainties associated with the perturbative matching or with neglecting higher order NRQCD terms are correlated between B and B_s simulations and therefore cancel in the ratio. The most precise result available for f_B takes advantage of these cancellations by combining a precise determination of the ratio f_B/f_{B_s} with the precise determination of f_{B_s} using HISQ b quarks to obtain $f_B = 0.189(4)$ GeV¹⁹. This result would have not been possible without LPT.

5.2. Heavy-heavy current renormalization

Heavy-heavy currents are required as part of the extraction of the CKM matrix element V_{cb} via exclusive semileptonic decays. The decay $B \rightarrow D^* \ell \nu$ is currently the most important exclusive process for attempts to reconcile the discrepancies between determinations of V_{cb} from inclusive and exclusive channels, but V_{cb} can also be extracted from $B \rightarrow D \ell \nu$. The BaBar collaboration recently reported an excess of 3.4σ above the expected Standard Model ratio $\text{BR}(B \rightarrow D^{(*)} \tau \nu)/\text{BR}(B \rightarrow D^{(*)} \ell \nu)$ in both channels¹²⁵, although a very recent lattice determination has reduced the tension to less than 2σ ²⁰.

Direct access to the CKM matrix element V_{cb} is possible through the leptonic decay $B_c \rightarrow \tau \nu$, which has decay rate

$$\Gamma(B_c \rightarrow \tau \nu) = \frac{G_F^2}{8\pi} |V_{cb}|^2 f_{B_c}^2 m_{B_c}^3 \frac{m_\tau}{m_{B_c}^2} \left(1 - \frac{m_\tau}{m_{B_c}}\right)^2, \quad (5)$$

where the decay constant is defined through

$$\langle 0 | A_0 | B_{(c)} \rangle = f_{B_{(c)}} M_{B_{(c)}}. \quad (6)$$

The experimental difficulties associated with reconstructing the τ lepton from its decay products are considerable¹²⁷ and this decay is yet to be observed experimentally. This, however, offers a unique possibility for lattice theorists: the prediction of the leptonic decay rate from lattice computations. Successful predictions lend significantly more weight to our belief in the validity of lattice results than postdictions and are an important aspect of testing lattice QCD.

Lattice determinations of the semileptonic $B \rightarrow D$ decays have so far been dominated by calculations from the Fermilab Lattice/MILC collaboration, which has studied various semileptonic B decays, including $B \rightarrow D \tau \nu$ ²⁰, $B \rightarrow D^* \ell \nu$ ¹²⁴ and the ratio of $\overline{B} \rightarrow D^+ \ell^- \overline{\nu}$ to $\overline{B}_s \rightarrow D_s^+ \ell^- \overline{\nu}$ ²¹. Calculations of both the semileptonic $B_{(s)} \rightarrow D_{(s)}$ and leptonic B_c decays are underway by the HPQCD collaboration.

Just as in the heavy-light sector, the role of LPT has been to determine matching coefficients for quark currents. The Fermilab Lattice/MILC collaboration's results for $B \rightarrow D$ processes required

the LPT heavy-heavy current matching calculations of ⁹⁷. The HPQCD collaboration is currently undertaking a determination of the matching coefficients required for the semileptonic $B_{(s)} \rightarrow D_{(s)}$ and leptonic B_c meson processes ¹¹⁵.

5.3. B mixing

The phenomenon of meson-antimeson oscillation is of particular interest to BSM physics hunters. Meson-antimeson mixing is a FCNC process and so, in the Standard Model, proceeds through one-loop box diagrams. This makes meson-antimeson mixing a particularly powerful constraint on both CKM unitarity and possible BSM physics.

Meson-antimeson mixing occurs in both the B_d^0 and B_s^0 systems and is primarily mediated by top quarks. Determinations of the oscillation frequencies, ΔM and ΔM_s respectively, directly constrain the CKM unitarity triangle through the Standard Model relations

$$\Delta M_q \propto |V_{tq}^* V_{tb}|^2 f_{B_q}^2 \widehat{B}_{B_q}, \quad (7)$$

where q may be either a d or s quark. Here the f_{B_q} are the decay constants discussed in the previous section and the \widehat{B}_{B_q} are the renormalization group invariant bag parameters. The decay constants and bag parameters parameterize the nonperturbative matrix elements defined by

$$\langle \overline{B}_q^0 | (\overline{q}\gamma^\mu(1-\gamma_5)b) (\overline{q}\gamma^\mu(1-\gamma_5)b) | B_q^0 \rangle = \frac{8}{3} M_{B_q}^2 f_{B_q}^2 B_{B_q}, \quad (8)$$

which are expressed in terms of the scale dependent bag parameters B_{B_q} . The relation between B_{B_q} and \widehat{B}_{B_q} is known perturbatively to next-to-leading order ^{128,129}.

Although both ΔM and ΔM_s directly constrain the apex of the CKM unitarity triangle, the SU(3) breaking ratio $\xi = f_{B_s} \sqrt{\widehat{B}_{B_s}} / f_{B_d} \sqrt{\widehat{B}_{B_d}}$ provides a more stringent bound on CKM matrix unitarity because many systematic uncertainties cancel in this ratio. New physics may couple to the B^0 and B_s^0 systems differently and so separate constraints from both ΔM and ΔM_s are required.

Precise determinations of the matrix elements in eq. (8) require lattice QCD. And extracting continuum results from these lattice computations is once again a job for LPT.

An exploratory study by the RBC/UKQCD collaboration found $\xi = 1.13(12)$ using a single lattice spacing on $n_f = 2 + 1$ dynamical domain wall configurations with static b quarks ¹³⁰. LPT was used to improve the axial-vector current and match the results to the continuum ^{131,132}. A more precise calculation by the HPQCD collaboration employed AsqTad light valence quarks and NRQCD b quarks on ensembles with $n_f = 2 + 1$ AsqTad sea quarks ¹³³. Using the perturbative matching results of ¹³⁴, the HPQCD collaboration obtained $\xi = 1.258(33)$. These results are currently being updated using the HISQ action for the light valence quarks, which should reduce the uncertainty. Most recently, the Fermilab Lattice/MILC collaboration found $\xi = 1.268(63)$ using the same $n_f = 2 + 1$ AsqTad configurations, with AsqTad light valence quarks and b quarks implemented with the Fermilab action. Details of the perturbative calculation required for this result are forthcoming.

5.4. b quark mass determinations

Although not directly measurable, the mass of the b quark is nevertheless an important object of study, both as a free parameter of the Standard Model and as an input into searches for BSM

physics.

The most precise nonperturbative result currently available for the b quark mass (expressed in the modified minimal subtraction, or \overline{MS} , scheme) is $m_{\overline{MS}}(m_{\overline{MS}}, n_f = 5) = 4.165(23)$ GeV, from a relativistic HISQ calculation by the HPQCD collaboration⁴⁶. Two different determinations using $n_f = 2$ ensembles from the ALPHA and ETM collaborations are in agreement with the results from heavy HISQ simulations. Using nonperturbatively tuned HQET, the ALPHA collaboration obtained a preliminary result of $m_{\overline{MS}}(m_{\overline{MS}}) = 4.22(10)(4)_z$ GeV¹¹¹, where the first error includes statistical and systematic uncertainties and the second arises from the quark mass renormalization. An alternative approach was taken by the ETM collaboration, using two different methods to find a (preliminary) average result of $m_{\overline{MS}}(m_{\overline{MS}}) = 4.29(13)_{\text{stat}}(4)_{\text{sys}}$ GeV²³. Here the first uncertainty is statistical and the second the total systematic uncertainty.

5.4.1. *A physics example: LPT in the HPQCD approach*

An example that illustrates the importance of LPT for precision B calculations is the extraction of the b quark mass from lattice NRQCD computations undertaken by the HPQCD collaboration. An early calculation obtained $m_{\overline{MS}}(m_{\overline{MS}}) = 4.4(3)$ GeV⁷⁵, where the uncertainty was dominated by the one-loop matching calculation needed to extract the continuum result. In recently completed work¹³⁶, the one-loop calculation was extended to two loops using a mixed approach combining automated LPT and weak coupling simulations to extract the heavy quark energy shift. Preliminary indications suggest that this will reduce the uncertainties to the sub percent level: a real vindication of the power of LPT for precision lattice NRQCD.

5.5. *Heavy meson spectroscopy*

My focus has so far been the application of LPT to precision tests of the Standard Model in the hunt for BSM physics. These efforts require precise theoretical calculations, which, for nonperturbative QCD, often means lattice computations. But how can we be sure that the precision of our computations really is improving and that we are not missing sources of systematic uncertainty?

To assuage these worries and to ensure that we really are improving the precision of our lattice calculations we need a proven testing ground for our results. In the B sector, this testing ground is heavy meson spectroscopy.

The heavy meson spectrum is an excellent arena for testing and quantifying uncertainties associated with lattice calculations¹³⁷. There are three reasons for this: firstly there are a number of gold-plated states that are experimentally and theoretically well defined; secondly there are multiple states that can be used as parameter-free tests of the current status of lattice calculations and their associated uncertainties; and thirdly and most importantly, there remain a number of experimentally undiscovered states that allow lattice QCD predictions to be tested. Predictions have considerably more credibility than postdictions and provide the most stringent tests of lattice computations.

An early vindication of the methods of precision lattice QCD occurred in the “prediction” of the B_c meson mass. Although this mass was reconstructed with a precision of about 400 MeV by the CDF collaboration in 1998¹²⁶, the resolution was sufficiently poor that a later lattice calculation could claim a “prediction” of $m_{B_c} = 6304 \pm 12^{+18}_0$ MeV¹³⁸. This result was confirmed

by observations at the Tevatron by the CDF collaboration¹³⁹ and the current world average value is $m_{B_c} = 6.277 \pm 0.006$ MeV¹¹. The HPQCD recently updated its result to 6.280 ± 10 MeV¹⁴⁰, in excellent agreement with the experimental value.

Heavy quark spectroscopy remains an important proving ground for lattice computations. The HPQCD collaboration has pioneered precision B spectroscopy using the HISQ action for light valence quarks and NRQCD b quarks. This programme spans accurate postdictions for both heavy-light and heavy-heavy systems^{18,140} and precise predictions, such as the mass of the vector B_c^* meson¹⁴¹, the spectra for excited B_c states¹⁴² or the D -wave spectra of the Υ ¹⁷. The current status of the B spectrum from the HPQCD collaboration is illustrated in Fig. 5.5.

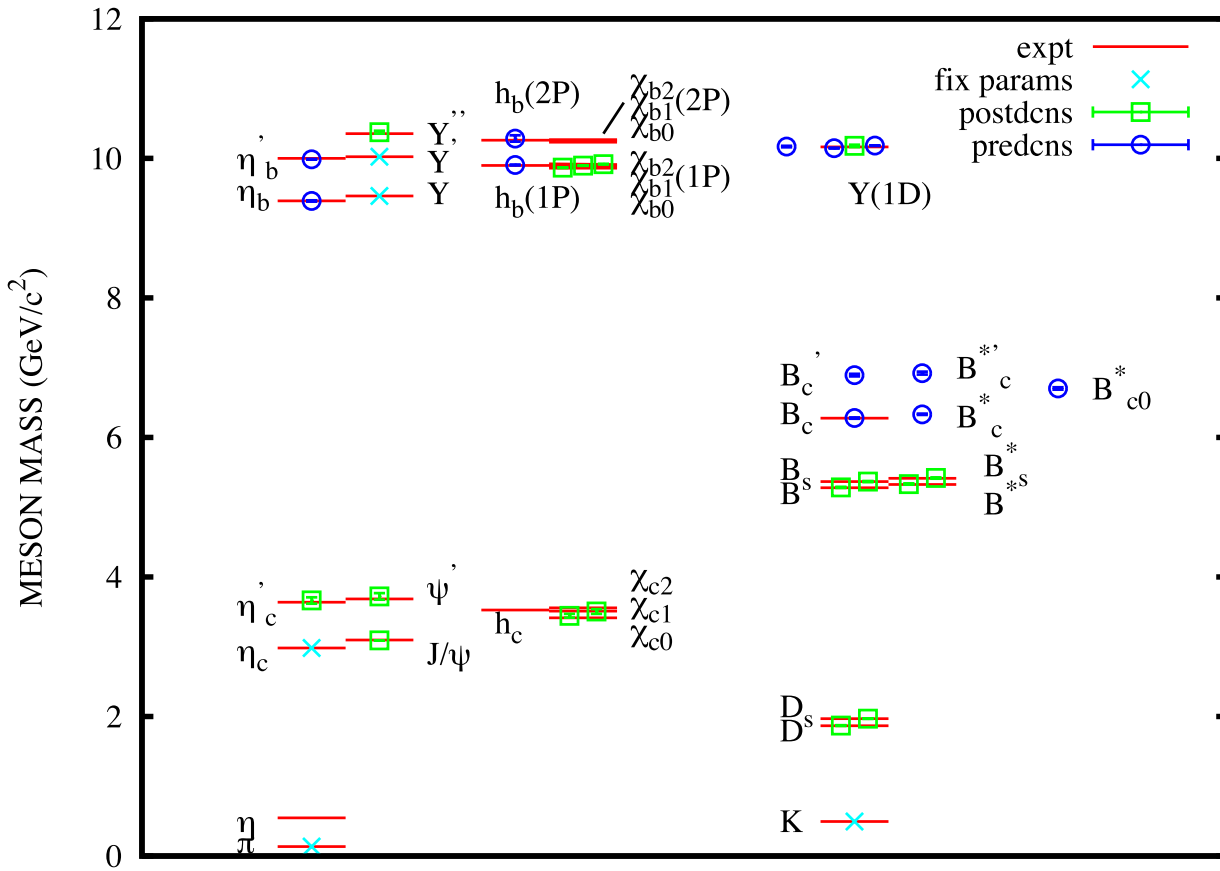


Fig. 2. The current status of precision B spectroscopy by the HPQCD collaboration. Figure reproduced courtesy of R.J. Dowdall *et al.*¹⁴.

The Fermilab Lattice/MILC collaboration has addressed heavy quark spectroscopy in^{93,143}, whilst the RBC/UKQCD collaboration has used relativistic heavy quarks to examine the low-lying heavy-heavy bound states⁴¹. The ETM and ALPHA collaborations are also currently undertaking calculations to address B spectroscopy. For heavy-heavy systems the spectrum and radiative decays of excited Υ states have recently been computed^{144,145,146}. Work has also been carried out on

triply-heavy b baryon spectroscopy, including not only the ground states^{147,148}, but even the excited states¹⁴⁹.

5.5.1. *A physics example: LPT in the HPQCD approach*

In the context of precision heavy meson spectroscopy, LPT has been primarily used to improve heavy quarks actions. The importance of this apparently small role is well illustrated by recent work on the hyperfine splitting of the Υ meson from lattice NRQCD¹⁸. In early determinations of this splitting, the HPQCD collaboration used a tree-level value of the coefficient of the chromomagnetic interaction in the NRQCD action⁷⁵. The results were not in good agreement with experimental data. A perturbative calculation of the one-loop correction to the chromo-magnetic interaction in NRQCD brought the lattice results in line with those from experiment⁶⁵. This calculation demonstrates the effectiveness of the Symanzik improvement programme for lattice NRQCD and perfectly illustrates the importance of LPT to precision B physics.

6. Conclusions

The past decade has heralded a range of impressive successes for B physics on the lattice. Precise predictions and accurate postdictions, particularly in B spectroscopy, have convincingly demonstrated the effectiveness of contemporary lattice calculations. Improving determinations of decay constants and form factors have facilitated ever-tightening constraints on the unitarity of the CKM matrix and placed more stringent bounds on BSM physics effects in rare B decays.

As more experimental data arrive, particularly from the LHC, further improvements and greater precision will be required from lattice computations. A close look at recent lattice QCD calculations reveals that lattice perturbation theory has been crucial in the development of precise theoretical results. A spectrum of applications of lattice perturbation theory can be found in contemporary lattice calculations, from the explicit — matching calculations used to extract continuum results — to the more implicit — in constructing, developing or improving lattice actions. Lattice perturbation theory has a home in the work of all the major lattice collaborations and will continue to help clarify our understanding of B physics.

Acknowledgments

I would like to thank Dirk Hesse and Christoph Lehner for useful discussions and helpful corrections regarding their automated LPT routines. Particular thanks go to Matthew Wingate for reading an early draft of the manuscript. This work has been partially supported by U.S. DOE Grant No. DE-FG02-04ER41302.

References

1. J. Albrecht, submitted to *Mod. Phys. Lett. A* (2012), [arXiv:1207.4287]
2. A.J. Buras *et al.* (2012), [arXiv:1208.0934]
3. R. Aaij *et al.*, (**LHCb**) *Phys. Rev. Lett.* **108**, 231801 (2012), [arXiv:1203.4493]
4. G. Aad *et al.*, (**ATLAS**) *Phys. Lett. B* **713**, 387 (2012), [arXiv:1204.0735]
5. S. Chatrchyan *et al.* (**CMS**) (2012), [arXiv:1203.3976]

6. D. Becirevic, *et al.* (2012), [arXiv:1209.0969]
7. R. Aaij *et al.* (**LHCb**), *JHEP* **1207**, 133 (2012), [arXiv:1205.3422]
8. J.P. Lees *et al.* (**BaBar**) (2012), [arXiv:1204.3933]
9. E. Lunghi and A. Soni, *Phys. Lett. B* **697**, 323 (2011), [arXiv:1010.6069]
10. J. Laiho, E. Lunghi and R.S. Van de Water, *PoS LAT2011* (2011), [arXiv:1204.0791]
11. J. Beringer *et al.* (**Particle Data Group**), *Phys. Rev. D* **86**, 010001 (2012)
12. J. Charles *et al.* (**CKMfitter**), *Eur. Phys. J. C* **41**, 1 (2005), [arXiv:hep-ph/0406184], updated results and plots available at: ckmfitter
13. (**UTfit**) utfit.org
14. W. Altmannshofer and D.M. Straub (2012), [arXiv:1206.0273]
15. W. Altmannshofer, P. Paradisi and D.M. Straub (2011), [arXiv:1111.1257]
16. C. Bobeth, G. Hiller and D. van Dyk, *JHEP* **1007**, 098 (2010), [arXiv:1006.5013]
17. J.O. Daldrop, C.T.H. Davies and R.J. Dowdall (**HPQCD**), *Phys. Rev. Lett.* **108**, 102003 (2011), [arXiv:1112.2590]
18. R.J. Dowdall *et al.* (**HPQCD**), *Phys. Rev. D* **85**, 054509 (2012), [arXiv:1110.6887]
19. H. Na *et al.* (**HPQCD**), *Phys. Rev. D* **86**, 034506 (2012), [arXiv:1202.4914]
20. J.A. Bailey *et al.* (**Fermilab Lattice/MILC**), *Phys. Rev. Lett.* **109** 071802 (2012), [arXiv:1206.4992]
21. J.A. Bailey *et al.* (**Fermilab Lattice/MILC**), *Phys. Rev. D* **85**, 114502 (2012), [arXiv:1202.6346]
22. A. Bazavov *et al.* (**Fermilab Lattice/MILC**), *Phys. Rev. D* **86**, 034503 (2012), [arXiv:1205.7013]
23. P. Dimopoulos *et al.* (**ETM**), *JHEP* **01**, 46 (2012), [arXiv:1107.1441]
24. B. Blossier *et al.* (**ALPHA**), (2010), [arXiv:1012.1357]
25. B. Blossier *et al.* (**ALPHA**), (2011), [arXiv:1112.6175]
26. G.P. Lepage, (1996), [arXiv:hep-lat/9607076]
27. G.P. Lepage *et al.*, *Nucl. Phys. (Proc. Suppl.)* **83**, 866 (2000), [arXiv:hep-lat/9910018]
28. F. Di Renzo and L. Scorzato, *JHEP* **10**, 038 (2001), [arXiv:hep-lat/0011067]
29. R. Horsley, P.E.L. Rakow and G. Scheierholz, *Nucl. Phys. (Proc. Suppl.)* **106**, 870 (2002)
30. H.D. Trottier *et al.*, *Phys. Rev. D* **65**, 094502 (2002), [arXiv:hep-lat/0111028]
31. A.G. Hart, R.R. Horgan and L.C. Stononi, *Phys. Rev. D* **70**, 034501 (2004), [arXiv:hep-lat/0402033]
32. K.Y. Wong, H.D. Trottier and R.M. Woloshyn, *Phys. Rev. D* **73**, 094512 (2006), [arXiv:hep-lat/0512012]

33. I.F. Allison *et al.* (**HPQCD**), *PoS LAT2008* 225 (2008), [arXiv:0810.0285]
34. G.P. Lepage and P.B. Mackenzie, *Phys. Rev. D* **48**, 2250 (1993)
35. S.J. Brodsky, G.P. Lepage and P.B. Mackenzie, *Phys. Rev. D* **28**, 228 (1983)
36. K. Hornbostel, G.P. Lepage and C. Morningstar, *Phys. Rev. D* **67**, 034023 (2002)
37. M. Lüscher, P. Weisz and U. Wolff, *Nucl. Phys. B* **359**, 221 (1991)
38. G. Martinelli *et al.*, *Nucl. Phys. B* **445**, 81 (1995), [arXiv:hep-lat/9411010]
39. H.-W. Lin and N.H. Christ, *Phys. Rev. D* **76**, 074506 (2007), [arXiv:hep-lat/0608005]
40. M. Lüscher *et al.*, *Nucl. Phys. B* **478**, 365 (1996), [arXiv:hep-lat/9605038]
41. Y. Aoki *et al.*, (2012), [arXiv:1206.2554]
42. M.A. Nobes *et al.*, *Nucl. Phys. (Proc. Suppl.)* **106**, 838 (2002), [arXiv:hep-lat/0110051]
43. Q. Mason, H.D. Trottier and R.R. Horgan, *PoS LAT2005* 011 (2005), [arXiv:hep-lat/0510053]
44. Q. Mason *et al.*, *Phys. Rev. D* **73**, 114501 (2005), [arXiv:hep-ph/0511160]
45. A.G. Hart *et al.*, *PoS LAT2010* 223 (2010), [arXiv:1010.6238]
46. C. McNeile *et al.* (**HPQCD**), *Phys. Rev. D* **82**, 034512 (2010), [arXiv:1004.4285]
47. C. McNeile *et al.* (**HPQCD**), *Phys. Rev. D* **85**, 031503 (2012), [arXiv:1110.4510]
48. C. McNeile *et al.* (**HPQCD**), (2012), [arXiv:1207.0994]
49. K. Symanzik, *Nucl. Phys. B* **226**, 187 (1983)
50. K. Symanzik, *Nucl. Phys. B* **226**, 205 (1983)
51. M. Lüscher and P. Weisz, *Nucl. Phys. B* **266**, 309 (1986)
52. M.A. Nobes and H.D. Trottier, *Nucl. Phys. (Proc. Suppl.)* **119**, 463 (2003) [arXiv:hep-lat/0209017]

53. M.A. Nobes and H.D. Trottier, *Nucl. Phys. (Proc. Suppl.)* **129**, 355 (2004) [arXiv:hep-lat/0309086]
54. A.G. Hart *et al.*, *J. Comput. Phys.* **209**, 340 (2005), [arXiv:hep-lat/0411026]
55. A.G. Hart *et al.*, *Comput. Phys. Commun.* **180**, 2698 (2009), [arXiv:0904.0375]
56. S. Takeda, *Nucl. Phys. B* **811**, 36 (2009), [arXiv:0808.3065]
57. D. Hesse, R. Sommer and G.M. von Hippel *PoS LAT2011*, 229 (2011)
58. D. Hesse, (2012), [arXiv:1211.5750]
59. D. Hesse and R. Sommer, (2012), [arXiv:1211.0866]
60. C. Lehner, (2012), [arXiv:1211.4013]
61. A.G. Hart, G.M. von Hippel and R.R. Horgan, *Phys. Rev. D* **75**, 014008 (2007), [arXiv:hep-lat/0609002]
62. E.H. Müller, A.G. Hart and R.R. Horgan, *Phys. Rev. D* **83**, 034501 (2011), [arXiv:1011.1215]
63. I.T. Drummond *et al.*, *Phys. Rev. D* **66**, 094509 (2002), [arXiv:hep-lat/0208010]
64. I.T. Drummond *et al.*, *Phys. Rev. D* **68**, 057501 (2003), [arXiv:hep-lat/0307010]
65. T.C. Hammant *et al.*, *Phys. Rev. Lett.* **107**, 112002 (2011), [arXiv:1105.5309]
66. G.P. Lepage, *CLNS-80/447* (1980)
67. G.M. von Hippel, *Comput. Phys. Commun.* **181**, 705 (2010), [arXiv:0910.5111]
68. G. Passarino and M.J.G. Veltman, *Nucl. Phys. B* **160**, 151 (1979)
69. E. Braaten, (1997), [arXiv:hep-lat/9702225]
70. M. Neubert, *Phys. Rep.* **245**, 259 (1994), [arXiv:hep-lat/9306320]
71. A.V. Manohar and M.V. Wise, *Heavy Quark Physics* (CUP, 2000)
72. A.G. Grozin, *Heavy Quark Effective Theory* (Springer, 2004)
73. R. Sommer, (2010), [arXiv:1008.0710]
74. C. Itzykson and J-B. Zuber, *Quantum Field Theory* (Dover,1980)
75. A. Gray *et al.* (**HPQCD**), *Phys. Rev. D* **72**, 094507 (2005) [arXiv:hep-lat/0507013]
76. T.C. Hammant *Quarks, Ions, DNA and Poker: Applications of Statistical Mechanics*, Ph.D. Thesis, University of Cambridge (2012)
77. J. Heitger and R. Sommer, *JHEP* **0402**, 022 (2004), [arXiv:hep-lat/0310035]
78. S. Bekavac *et al.*, *Nucl. Phys. B* **833**, 46 (2010)
79. C. Sachrajda, *Nucl. Phys. B (Proc. Suppl.)* **47**, 100 (1996)
80. M. Beneke, *Phys. Reports* **317**, 1 (1999), [arXiv:hep-ph/9807443]
81. A. Grozin (2003), [arXiv:hep-ph/0311050]
82. I.I. Bigi *et al.* *Phys. Rev. D* **50**, 2234 (1994)
83. M. Beneke and V.M. Braun, *Nucl. Phys. B* **426**, 301 (1994)
84. M. Della Morte *et al.* (**ALPHA**), *JHEP* **0701**, 007 (2007), [arXiv:hep-ph/0609294]
85. B. Blossier *et al.* (**ALPHA**), *JHEP* **1005**, 074 (2010), [arXiv:1004.2661]
86. B. Blossier *et al.* (**ALPHA**), *JHEP* **1012**, 038 (2010), [arXiv:1006.5816]
87. B. Blossier *et al.* (**ALPHA**), *JHEP* **1006**, 002 (2010), [arXiv:1001.4783]
88. B. Blossier *et al.* (**ALPHA**), (2012), [arXiv:1203.6516]
89. A.X. El-Khadra, A.S. Kronfeld and P.B. Mackenzie, *Phys. Rev. D* **55**, 3922 (1997), [arXiv:hep-lat/9604004]
90. S. Aoki, Y. Kuramashi and S. Tominaga, *Prog. Theor. Phys.* **109**, 383 (2003), [arXiv:hep-lat/0107009]
91. N.H. Christ, M. Li and H.-W. Lin, *Phys. Rev. D* **76**, 074505 (2007), [arXiv:hep-lat/0608006]
92. B. Sheikholeslami and R. Wohlert, *Nucl. Phys. B* **259**, 572 (1985)
93. C. Bernard *et al.* (**Fermilab Lattice/MILC**), *Phys. Rev. D* **83**, 034503 (2011), [arXiv:1003.1937]
94. J. Harada *et al.*, *Phys. Rev. D* **65**, 094513 (2002), [arXiv:hep-lat/0112044]
95. J. Harada *et al.*, *Phys. Rev. D* **65**, 094515 (2002), [arXiv:hep-lat/0112045]
96. J. Harada *et al.* *Phys. Rev. D* **71**, 019903(E) (2005), [arXiv:hep-lat/0112044]
97. A.X. El-Khadra *et al.*, *Pos LAT2007* 242, (2007), [arXiv:0710.1437]
98. S. Aoki, Y. Kayaba and Y. Kuramashi, *Nucl. Phys. B* **697**, 271 (2004), [arXiv:hep-lat/0309161]
99. B. Blossier *et al.* (**ETM**), *PoS LATT* 151 (2009), [arXiv:0911.3757]
100. B. Blossier *et al.* (**ETM**), *JHEP* **1004**, 049 (2010), [arXiv:0909.3187]

101. E. Follana *et al.* (**HPQCD**) *Phys. Rev. D* **75**, 054502 (2007) [arXiv:hep-lat/0610092]
102. M. Constantinou *et al.* (**ETM**) *JHEP* **1008**, 068 (2010), [arXiv:1004.1115]
103. M. Constantinou *et al.*, (2011), [arXiv:1210.7737]
104. M. Constantinou *et al.* (**ETM**), *JHEP* **0910**, 064 (2009), [arXiv:0907.0381]
105. M. Wingate, *Mod. Phys. Lett. A* **21**, 1167 (2006) [arXiv:hep-ph/0604254]
106. C. Bouchard *et al.* (**HPQCD**), [arXiv:1210.6992] (2012)
107. C. Bozzi *et al.* (**LHCb**), *LHCb results on semileptonic $B/B_s/\Lambda_b$ decays*, Talk presented at CKM 2012 (2012)
108. P. Urquijo, *B_s semileptonic experiment (sans LHCb) mini-review*, Talk presented at CKM 2012 (2012)
109. J.P. Lees *et al.* (**BaBar**), (2012), arXiv:1207.0698
110. A.J. Buras, *Phys. Lett. B* **566**, 115 (2003)
111. F. Bernardoni *et al.* (**ALPHA**), (2012), [arXiv:1210.6524]
112. F. Bahr *et al.* (2012), [arXiv:1210.3478]
113. J.A. Bailey *et al.* (**Fermilab Lattice/MILC**) *Phys. Rev. D* **79**, 054507 (2009), [arXiv:0811.3640]
114. A. Bazavov *et al.* (**Fermilab Lattice/MILC**), (2012), [arXiv:1112.3051]
115. C.J. Monahan *et al.* (**HPQCD**), (2012), [arXiv:1210.7016]
116. E. Gulez *et al.* (**HPQCD**), *Phys. Rev. D* **73**, 074502 (2006), [arXiv:hep-lat/0601021]
117. E. Gulez *et al.* (**HPQCD**), *Phys. Rev. D* **75**, 119906(E) (2007), [arXiv:hep-lat/0601021]
118. Y. Kuramashi, *Phys. Rev. D* **58**, 034507 (1998), [arXiv:hep-lat/9705036]
119. E. Braaten and S. Fleming, *Phys. Rev. D* **52**, 181 (1995)
120. P. Boyle and C.T.H. Davies, *Phys. Rev. D* **62**, 074507 (2000), [arXiv:hep-lat/0003026]
121. C.J. Morningstar and J. Shigemitsu, *Phys. Rev. D* **57**, 6741 (1998), [arXiv:hep-lat/9712016]
122. C.J. Morningstar and J. Shigemitsu, *Phys. Rev. D* **59**, 094504 (1999), [arXiv:hep-lat/9810047]
123. E. Gulez, J. Shigemitsu and M. Wingate, *Phys. Rev. D* **69**, 074501 (2004), [arXiv:hep-lat/0409140]
124. C. Bernard *et al.* (**Fermilab Lattice/MILC**), *Phys. Rev. D* **79**, 014506 (2009), [arXiv:0808.2519]
125. J.P. Lees *et al.* (**BaBar**), *Phys. Rev. Lett.* **109**, 101802 (2012), arXiv:1205.5442
126. F. Abe *et al.* (**CDF**), *Phys. Rev. Lett.* **81**, 2432 (1998)
127. G. Chiladze, A.F. Falk and A.A. Petrov, *Phys. Rev. D* **60**, 034011 (1999), [arXiv:hep-ph/9811405]
128. M. Ciuchini *et al.*, *Nucl. Phys. B* **523**, 501 (1998), [arXiv:hep-ph/9711402]
129. A.J. Buras, M. Misiak and J. Urban, *Nucl. Phys. B* **586**, 397 (2000), [arXiv:hep-ph/0005183]
130. C. Albertus *et al.* (**RBC/UKQCD**), (2010), [arXiv:1001.2023]
131. O. Laktik and T. Izubuchi, *Phys. Rev. D* **75**, 034504 (2007), [arXiv:hep-lat/0612022]
132. N.H. Christ *et al.* (**RBC/UKQCD**), *PoS LAT2007* 351 (2007), [arXiv:0710.5283]
133. E. Gamiz *et al.* (**HPQCD**), *Phys. Rev. D* **80**, 014503 (2009) [arXiv:0902.1815]
134. E. Gamiz, J. Shigemitsu and H.D. Trottier, *Phys. Rev. D* **77**, 114505 (2008) [arXiv:0804.1557]
135. S. Hashimoto *et al.*, *Phys. Rev. D* **62** 114502 (2000) [arXiv:hep-lat/0004022]
136. A.J. Lee *et al.*, *in preparation* (2012)
137. C.T.H. Davies *et al.* **HPQCD/MILC/Fermilab Lattice/UKQCD**, *Phys. Rev. Lett.* **92**, 022001 (2004) [arXiv:hep-lat/0304004]
138. I.F. Allison *et al.* (**HPQCD/Fermilab Lattice/UKQCD**), *Phys. Rev. Lett.* **94**, 172001 (2005) [arXiv:hep-lat/0411027]
139. A. Abulencia *et al.* (**CDF**), *Phys. Rev. Lett.* **97**, 012002, (2006), arXiv:hep-ex/0603027
140. E.B. Gregory *et al.* (**HPQCD**), *Phys. Rev. D* **83**, 014506 (2011), [arXiv:1010.3848]
141. E.B. Gregory *et al.* (**HPQCD**), *Phys. Rev. Lett.* **104**, 022001, (2010) [arXiv:0909.4462]
142. R.J. Dowdall *et al.*, (2012), [arXiv:1207.5149]
143. T. Burch *et al.* (**Fermilab Lattice/MILC**), *Phys. Rev. D* **81**, 034508 (2010), [arXiv:0912.2701]
144. R. Lewis and R. Woloshyn, *Phys. Rev. D* **84**, 094501 (2011), [arXiv:1108.1137]
145. R. Lewis and R. Woloshyn, *Phys. Rev. D* **85**, 114509 (2012), [arXiv:1204.4075]
146. R. Lewis and R. Woloshyn, *Phys. Rev. D* **86**, 057501 (2012), [arXiv:1207.3825]
147. S. Meinel, *Phys. Rev. D* **82**, 114502 (2010), [arXiv:1007.3966]

148. S. Meinel, *Phys. Rev. D* **82**, 114514 (2010), [arXiv:1008.3154]
149. S. Meinel, *Phys. Rev. D* **85**, 114510 (2012), [arXiv:1202.1312]